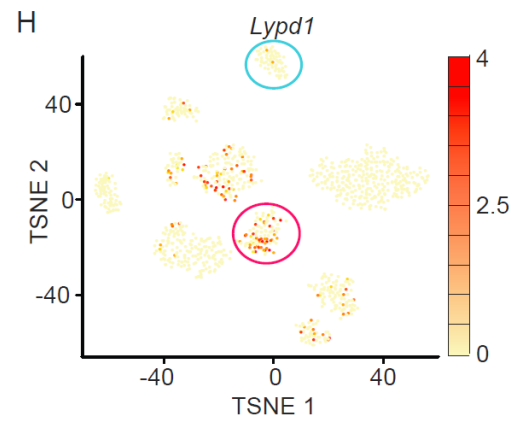
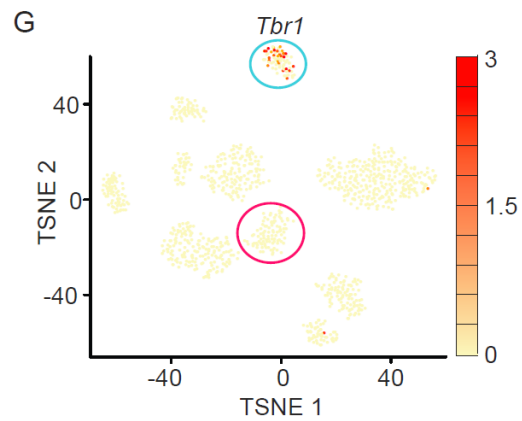
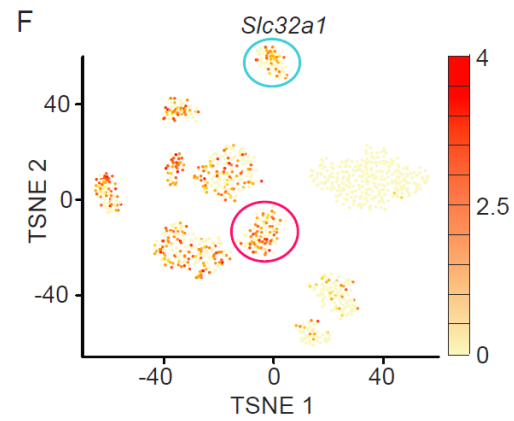
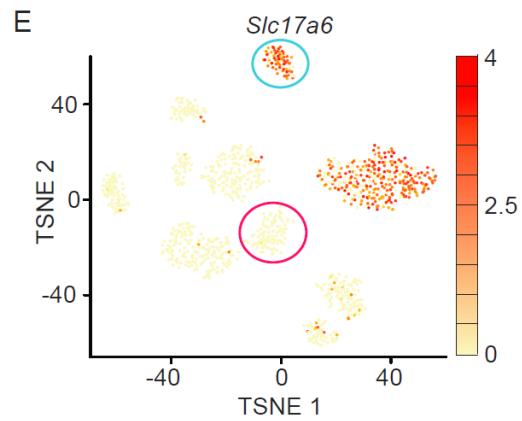
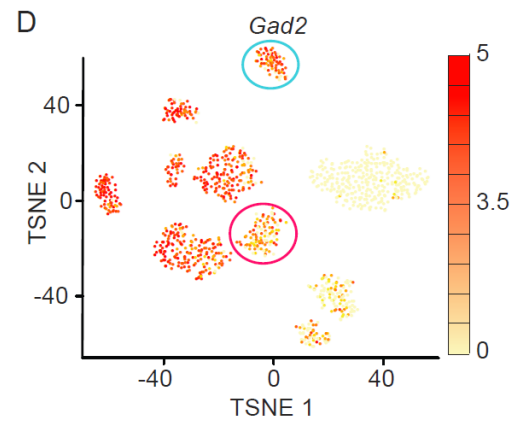
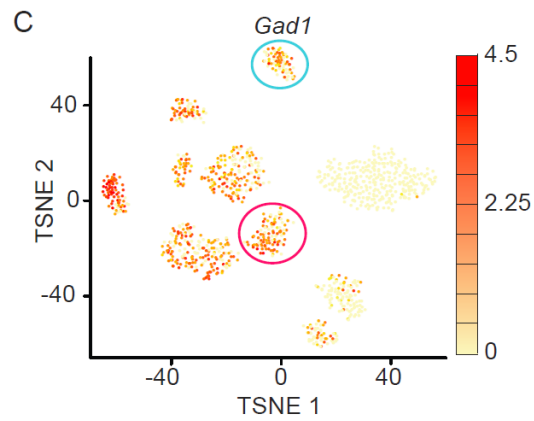
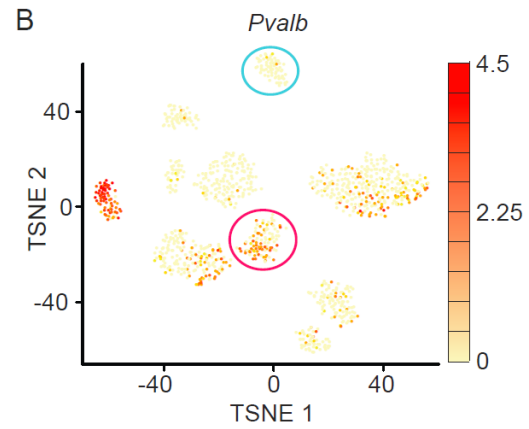
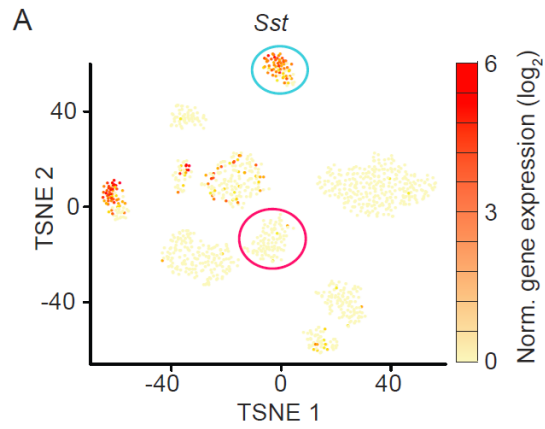


Supp. Fig. 1 (related to Figure 1 and 2)

Assignment of Drop-seq clusters to anatomical regions using differential gene expression and Allen Institute gene expression atlas

A. TSNE (t-distributed stochastic neighbor embedding) plot displaying the results of clustering of the 1,615 neurons sequenced from acute microdissections. **B,C.**

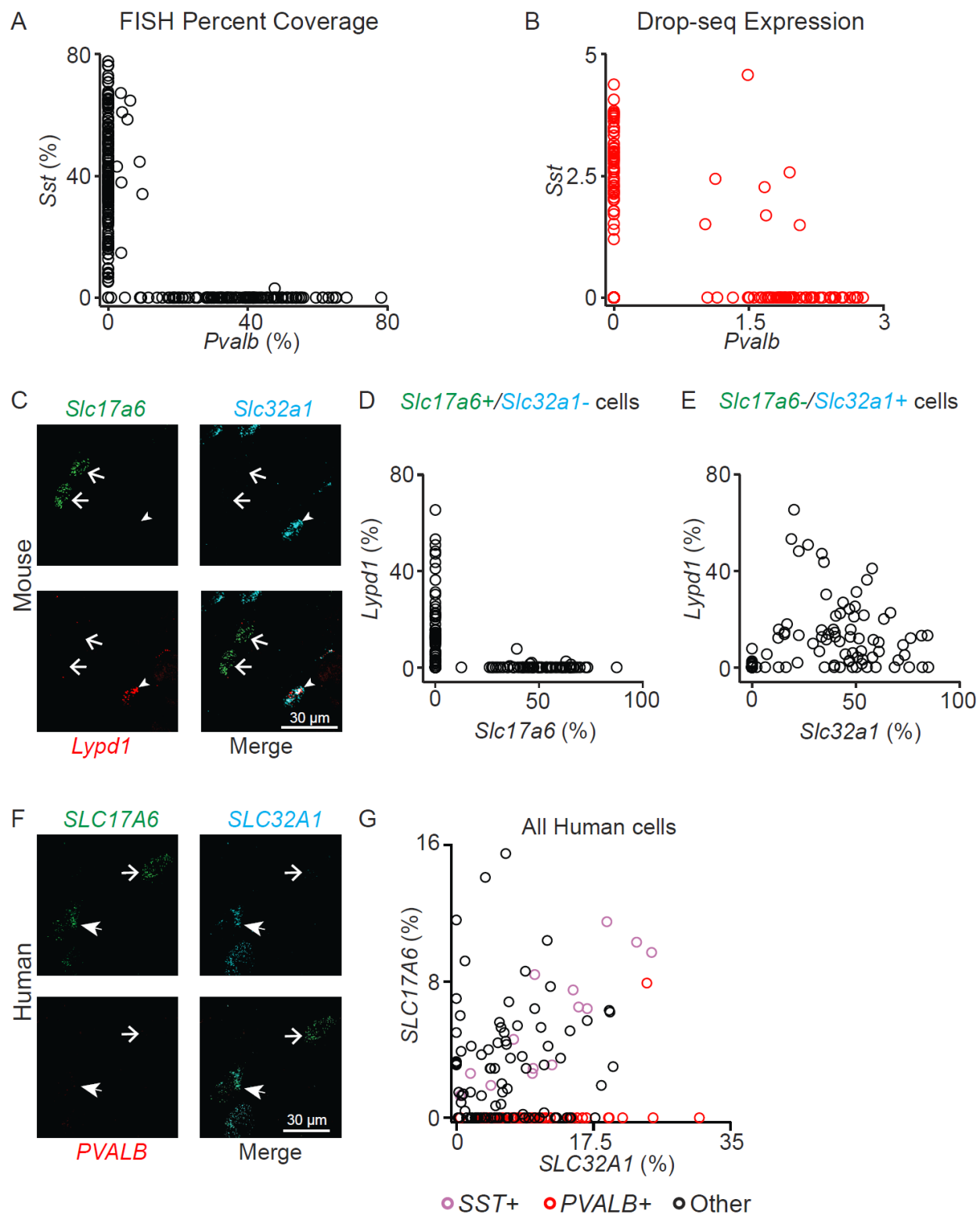
Expression of *Olig1* and *Snap25* overlaid on TSNE plot of all neurons analyzed. Expression of *Olig1* is highest and expression of *Snap25* is lowest in clusters 1 and 2, suggesting these clusters are not entirely neuronal (circled). Color scale to the right of TSNE plot denotes expression levels for each cell, expression levels are \log_2 normalized. **D.** Illustration of a sagittal section showing EP and surrounding regions, inset is region shown in subsequent RNA *in situ* hybridization (ISH) images. **E.** ISH (*left*) for *Pitx2* showing high expression in STN (outlined in gray) but not surrounding regions. (*right*) TSNE plot showing expression of *Pitx2* restricted to cluster 4. **F.** ISH (*left*) for *Meis2* showing high expression in vZI and (*right*) TSNE plot showing high expression of *Meis2* in cluster 7. **G.** ISH (*left*) for *Dlk1* showing high expression in dZI and (*right*) TSNE plot showing high expression of *Dlk1* in cluster 8. **H.** ISH (*left*) for *Ubash3b* showing high expression in TRN and (*right*) TSNE plot showing high expression of *Ubash3b* in cluster 9. **I.** ISH (*left*) for *Calb2* showing high expression in SI/L. Hypo and (*right*) TSNE plot showing high expression of *Calb2* in cluster 10 (TRN = thalamic reticular nucleus, ZId/v = zona incerta dorsal/ventral, STN = subthalamic nucleus, SI/L. Hypo. = substantia inominata/lateral hypothalamus). ***Note: The genes chosen for display in Figure S1 are examples of differentially expressed gene taken from the list in Table S1 and are representative of expression patterns seen for many other differentially expressed genes in each cluster.



Supp. Fig. 2 (related to Figure 1 and 2)

Single neuron mRNA expression levels of selected genes from all neurons.

A-H Relative expression levels of selected genes (*top of each panel*) in all neurons collected for Drop-seq analysis. Color scale to the right of TSNE plot denotes expression levels for each cell, expression levels are \log_2 normalized. EP clusters 5 (magenta) and 6 (blue) are circled.

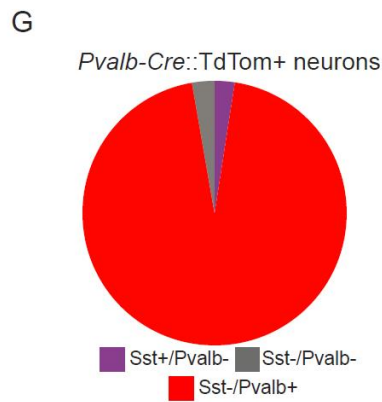
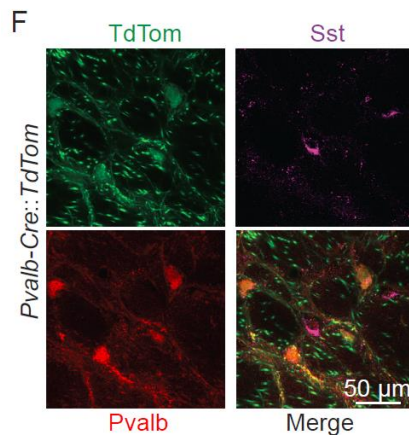
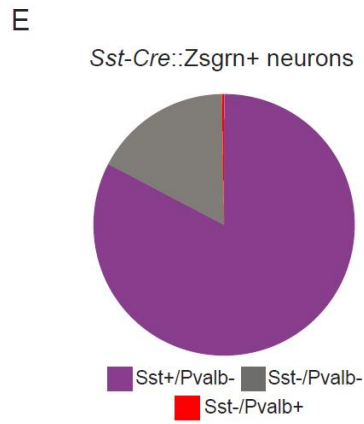
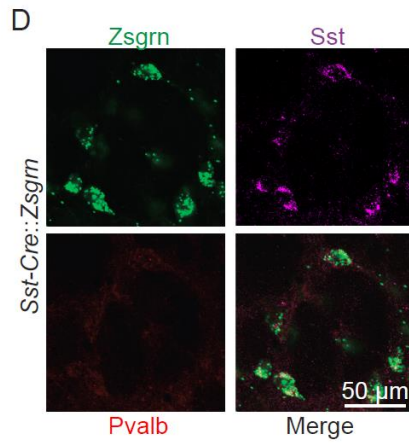
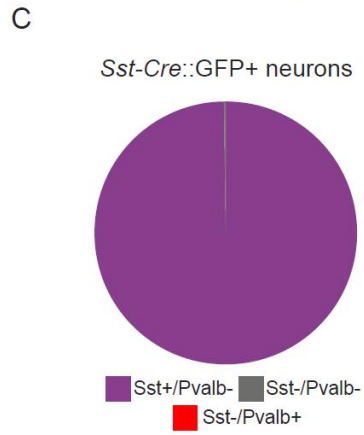
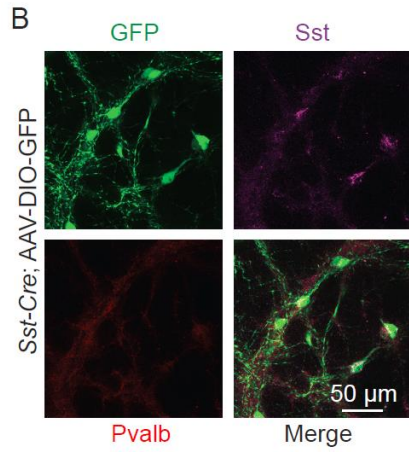
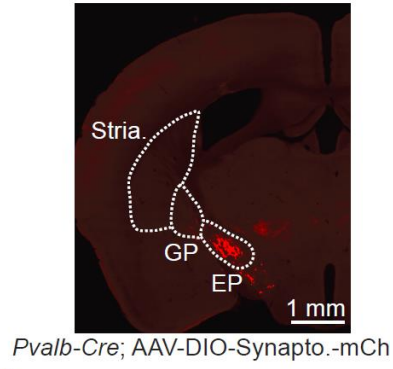
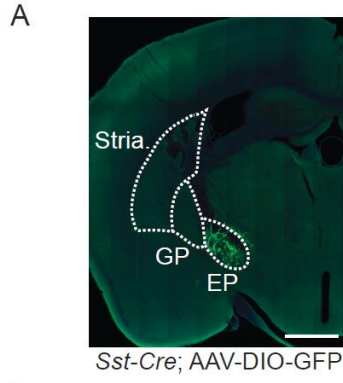


Supp. Fig.3 (related to Figure 1 and 3)

Comparison of single cell RNA expression levels in mouse EP and Human GPI

A, B. Comparison between fluorescence coverage of *Sst* and *Pvalb* using FISH (n=225)

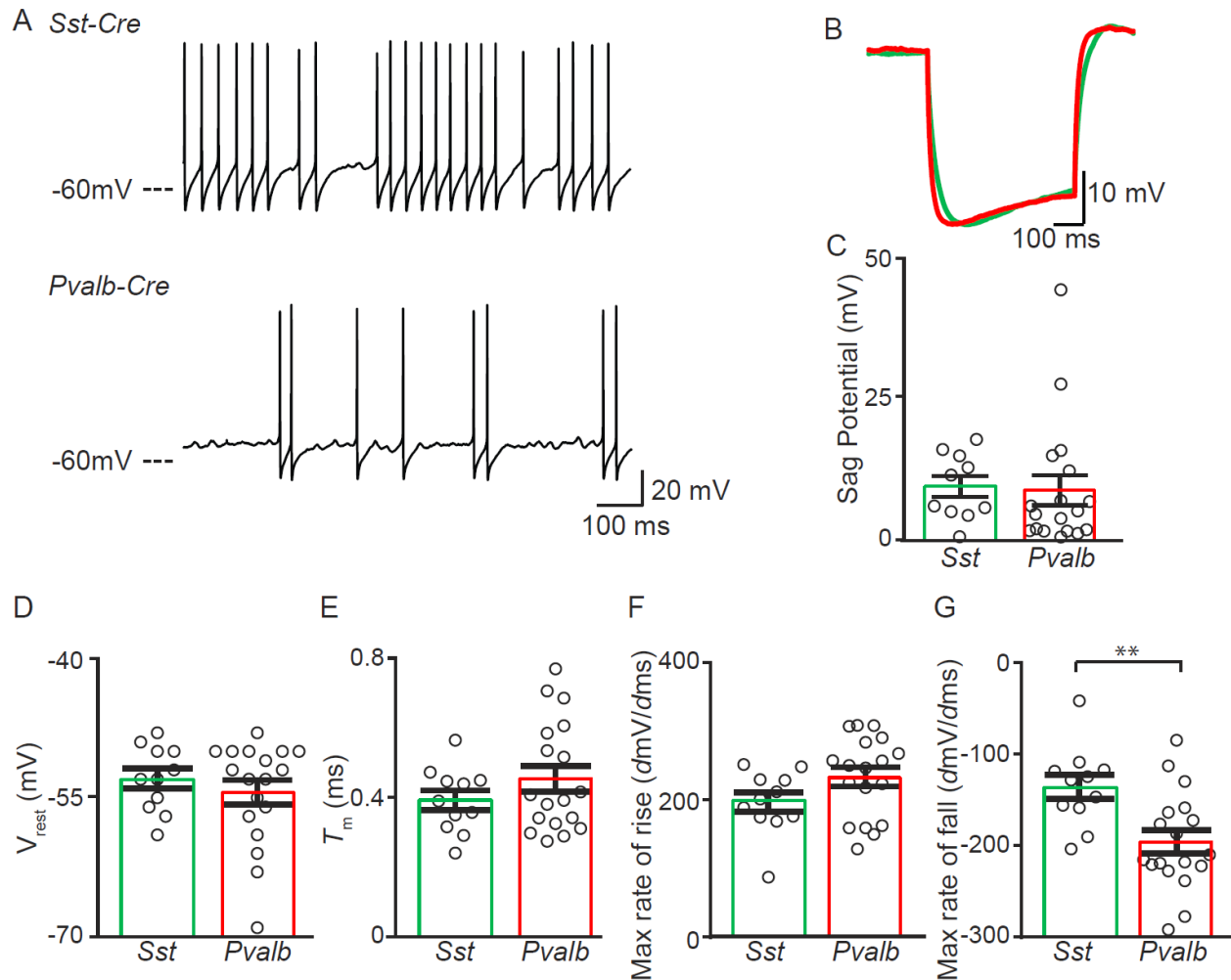
cells), and mRNA expression levels using Drop-seq (cells from clusters 5 and 6 combined, n=214 cells) in individual EP neurons. **C.** A sample image of a coronal section of EP probed for *Slc17a6* (green), *Slc32a1* (cyan), and *Lypd1* (red). Arrows point to *Slc17a6+*/*Slc32a1*-/*Lypd1*- EP neurons, arrowheads point to a *Slc17a6*-/*Slc32a1*+/*Lypd1*+ EP neuron. **D.** Quantification of fluorescence coverage of *Slc17a6* and *Lypd1* in *Slc17a6+*/*Slc32a1*- EP neurons. **E.** Quantification of fluorescence coverage of *Slc32a1* and *Lypd1* in *Slc17a6*-/*Slc32a1*+ EP neurons. **F.** A sample image of a coronal section of human GPi probed for *SLC17A6* (green), *SLC32A1* (cyan), and *PVALB* (red). Arrow points to *SLC17A6+*/*SLC32A1*- GPi neuron, arrowhead points to a *SLC17A6+*/*SLC32A1*+/*PVALB*- GPi neuron. **G.** Quantification of fluorescence coverage of *SLC32A1* and *SLC17A6* in all human GPi neurons, *SST*+ neurons are magenta and *PVALB*+ neurons are red.



Supp. Fig.4 (related to Figure 4)

Characterization of *Sst-Cre* and *Pvalb-Cre* mouse lines in EP.

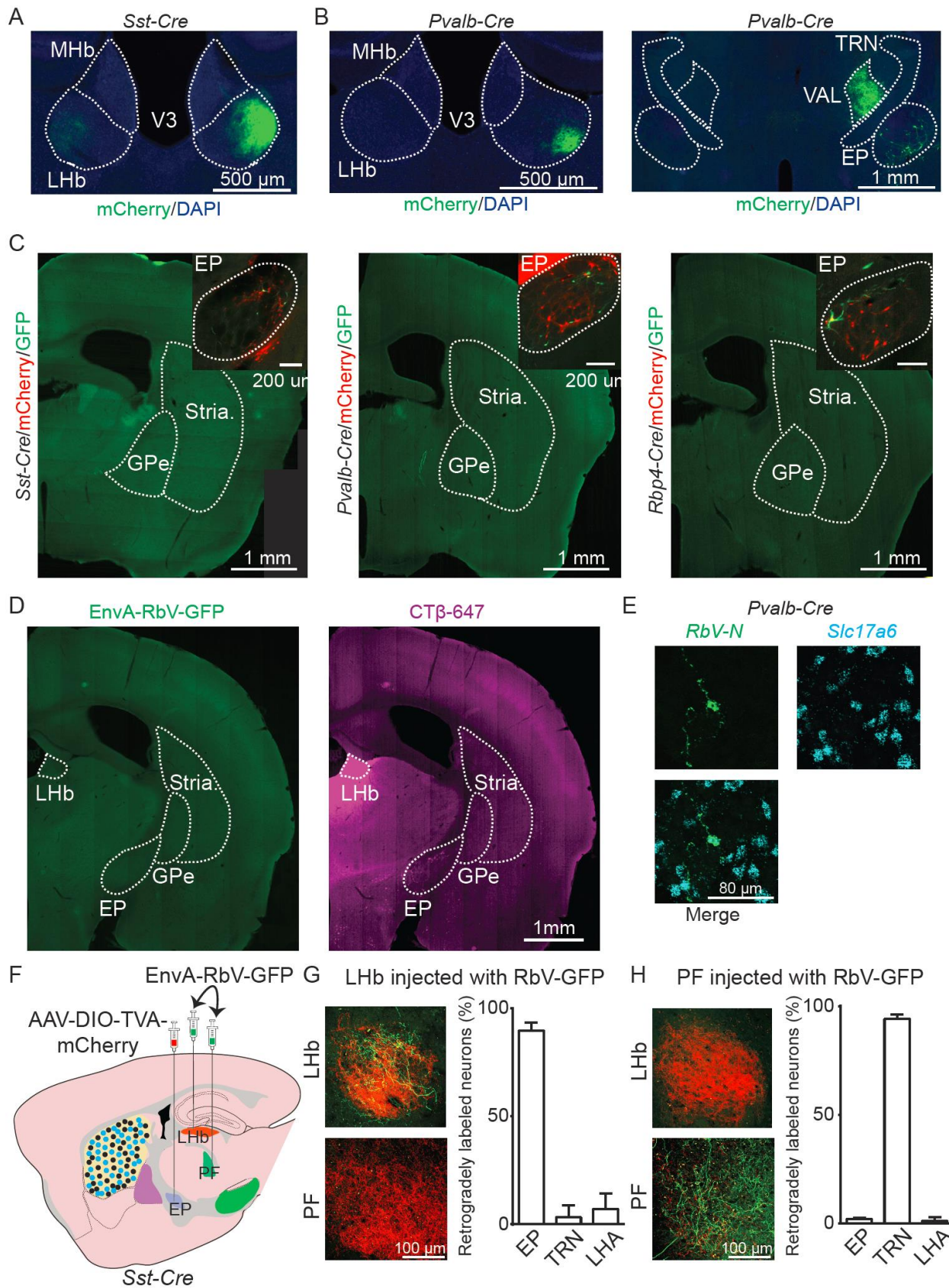
Both transgenic lines largely recapitulated endogenous protein expression patterns in EP, but *Sst-Cre* was slightly more specific when injected with a Cre-dependent virus in adulthood (B). **A.** Sample image of viral injections targeting EP in *Sst-Cre* (*left*) and *Pvalb-Cre* (*right*) mice. **B.** Sample image of *Sst-Cre::GFP+* (green) neurons in the EP immunostained for somatostatin (magenta) and parvalbumin (red). **C.** The proportion of GFP+ neurons that were immunolabeled for Somatostatin when adult *Sst-Cre* mice were intracranially injected in EP with a Cre-dependent adeno-associated virus (AAV) encoding GFP (881 of 883; n=2 mice; 99.7% of GFP+ neurons expressed Somatostatin). **D.** Sample image of *Sst-Cre::Zsgrn+* neurons in the EP immunostained for somatostatin (magenta) and parvalbumin (red). **E.** *Sst-IRES-Cre* (*Sst-Cre*) (Taniguchi et al., 2011) mice crossed to the fluorescent reporter (ZsGreen1 (*Zsgrn*); Ai6) mouse (Madisen et al., 2010) resulted in faithful labeling of Somatostatin+ neurons in the EP, while avoiding labeling of Parvalbumin positive neurons (301 of 364; n=2 mice; 82.6% of *Zsgrn+* neurons expressed Somatostatin; 1 of 364 expressed *Pvalb*). **F.** Sample image of *Pvalb-Cre::TdTom+* neurons in the EP immunostained for somatostatin (magenta) and parvalbumin (red). **G.** *Pvalb-IRES-Cre* (*Pvalb-Cre*) (Hippenmeyer et al., 2005) mice were crossed to a fluorescent reporter mouse (Ai14) expressing tdTomato in a Cre-dependent manner (Madisen et al., 2010) and recapitulated endogenous protein expression patterns in EP (346 of 365; n=3 mice; 94.7% of *tdTom+* neurons expressed Parvalbumin).



Supp. Fig.5 (related to Figure 4)

Spontaneous spiking, sag potential, and additional membrane and AP properties of EP neurons.

A. Current-clamp recordings of spontaneous spiking from *Sst-Cre*⁺ (top) and *Pvalb-Cre*⁺ (bottom) EP neurons. 9 of 11 (81%) *Sst-Cre*⁺ neurons, and 13 of 18 (72%) *Pvalb-Cre*⁺ neurons fired spontaneous action potentials at rest. **B, C.** Sample current-clamp recording of a response to a -100 pA square wave current injection (**B**) and sag potential measurements from *Sst-Cre* (green) and *Pvalb-Cre* (red) neurons (**C**). **D, E, F, G.** Resting membrane potential (V_{rest}), membrane time constant (T_m), max rate of rise, and max rate of fall of the action potential across EP cell types. All data are represented as mean \pm SEM, *= p <0.05.



Supp. Fig.6 (related to Figure 5)

Anatomical characterization of EP cell types and controls for EnvA-RbV-GFP

A. Sample image of mCherry+ (*green*) axons in the LHb of a *Sst-Cre* mouse injected unilaterally with TVA-mCherry in the right EP. Axons were observed bilaterally in LHb.

B. (*left*) Sample image of mCherry+ (*green*) axons in the LHb of a *Pvalb-Cre* mouse injected unilaterally with TVA-mCherry in the right EP. Axons were observed unilaterally in LHb. (*right*) Sample image of mCherry+ (*green*) axons in the VAL thalamus of a *Pvalb-Cre* mouse injected unilaterally with TVA-mCherry in the right EP. Axons were observed unilaterally in VAL thalamus.

C. Sample images of negative controls for rabies virus glycoprotein (G). Injections were performed as in Figure 7A, however AAV-DIO-G was omitted. Therefore, the rabies virus is unable to transfer to presynaptic cells and RbV-GFP+ neurons were not observed in the GPe or striatum.

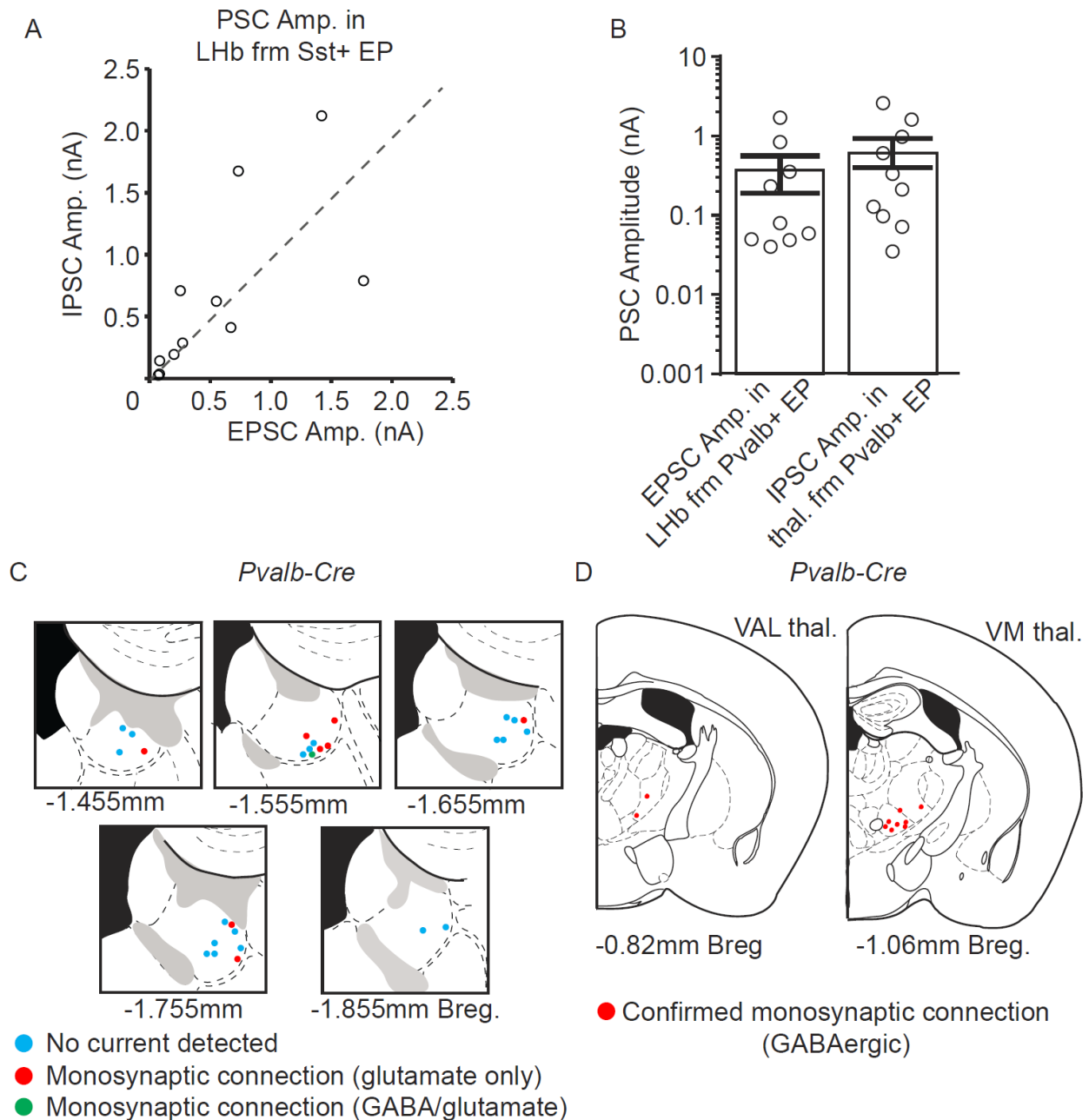
C. Sample images of a control experiment testing the requirement of TVA for expression EnvA-RbV-GFP. EnvA-RbV-GFP was coinjected into LHb with retrograde tracer CT β -647 (1 μ g/ μ L), but AAV-DIO-TVA-mCherry was *not* injected into EP. No GFP+ cells were observed, but CT β -647+ neurons were abundant in EP.

E. A sample image of a coronal section of EP probed for *RbV-N* (*green*) and *Slc17a6* (*cyan*), related to Figure 5H.

F. Illustration of a sagittal slice depicting AAV-DIO-TVA-mCherry viral injection in EP, and EnvA-RbV-GFP injection in either LHb (G) or PF (H) in a *Sst-Cre* mouse.

G. *left*, Images of LHb and PF depicting axonal labeling following EnvA-RbV-GFP (*green*) injection into LHb and TVA-mCherry (*red*) injection into EP. *right*, Quantification of neuronal soma location of retrogradely labeled neurons following EnvA-RbV-GFP injection into LHb (n=119 cells, 3 mice).

H. *left*, Images of LHb and PF depicting axonal labeling following EnvA-RbV-GFP (*green*) injection into PF and TVA-mCherry (*red*) injection into EP. *right*, Quantification of neuronal soma location of retrogradely labeled neurons following EnvA-RbV-GFP injection into PF (n=271 cells, 2 mice). All data are represented as mean \pm SEM.



Supp. Fig.7 (related to Figure 6)

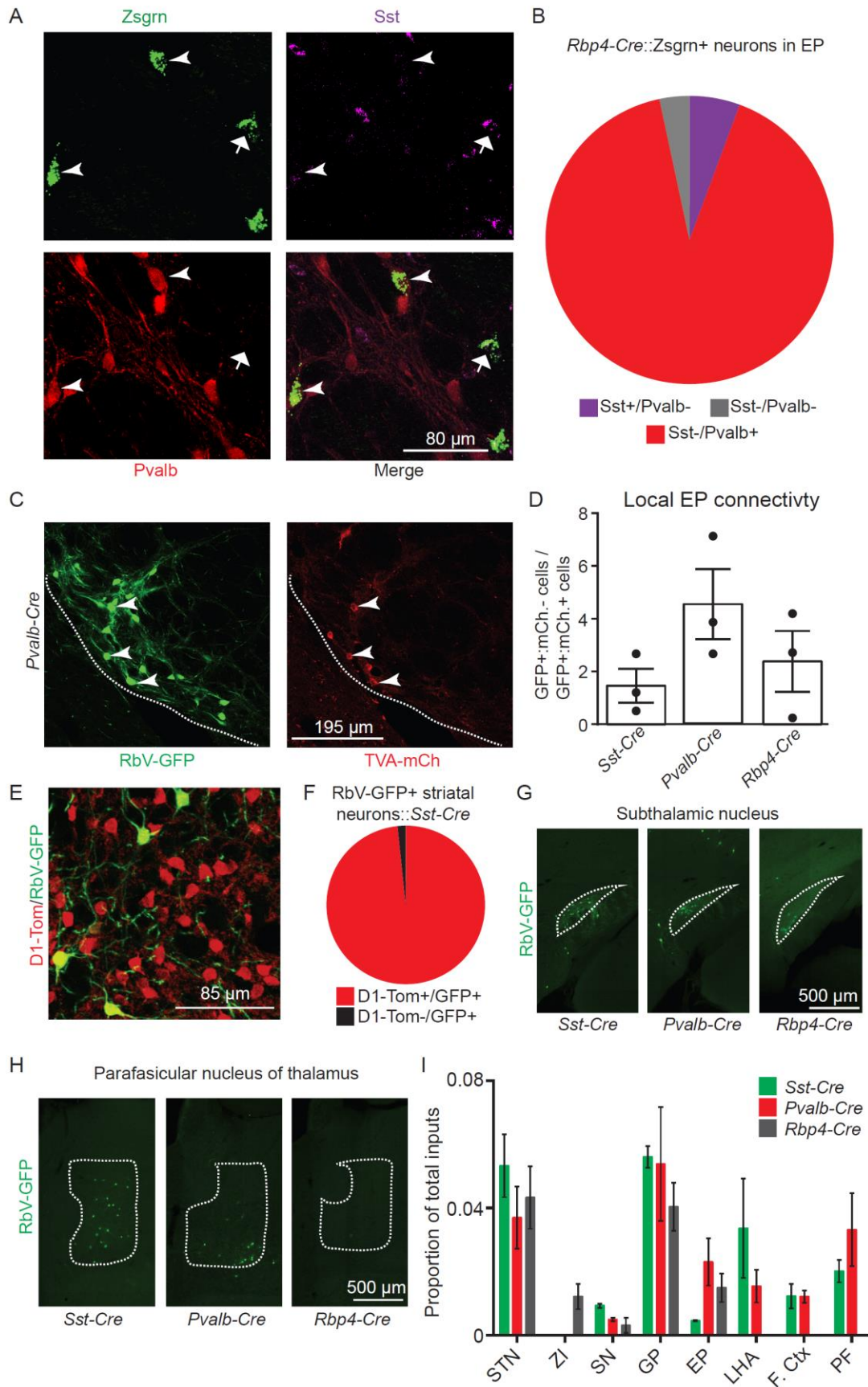
Raw oEPSC/IPSC amplitudes and recording locations from *Pvalb-Cre* mice

A. Raw IPSC and EPSC amplitudes recorded in single LHB neurons following optogenetic stimulation of *Sst-Cre*+ EP axons. EPSCs were recorded in the presence of TTX and 4-AP at -75mV and IPSCs were recorded in the presence of TTX, 4-AP, NBQX, and CPP at 0mV (n=11 cells). **B.** Monosynaptic optogenetically evoked PSC amplitudes from *Pvalb*+ EP neurons to two different target regions (LHB and VM/VAL). Currents were recorded in the presence of TTX and 4-AP. **C.** Locations of recordings in

LHb following AAV-DIO-ChR2-mCh. injection into the EP of a *Pvalb-Cre* mouse. **D.**

Locations of recordings in VAL and VM thalamus following AAV-DIO-ChR2-mCh.

injection into the EP of a *Pvalb-Cre* mouse. All data are represented as mean \pm SEM.



Supp. Fig.8 (related to Figure 7 and 8)

***Rbp4-Cre* characterization, intra-EP trans-synaptic tracing, molecular characterization of presynaptically labeled striatal neurons, and whole brain quantification of monosynaptic retrograde tracing.**

A. Sample image of *Rbp4-Cre::Zsgrn+* neurons in the EP immunostained for somatostatin (magenta) and parvalbumin (red). Arrowheads demarcate *Pvalb+::Zsgrn+* neurons and arrows demarcate *Sst+::Zsgrn+* neurons **B.** Quantification of *Rbp4-Cre::Zsgrn+* neurons in EP, 90% of *Zsgrn+* cells (434/477 cells) are also positive for *Pvalb*. **C.** Sample image of EP neurons infected in EP with AAV-DIO-TVA-mCherry/AAV-DIO-G (right) and in LHb with EnvA-RbV-GFP (left) in a *Pvalb-Cre* mouse. Arrowheads demarcate a subset of neurons that are positive for TVA-mCherry and RbV-GFP and are considered “starter” neurons. Neurons that are GFP+ only are putative presynaptic neurons labeled locally within the EP. **D.** Quantification of the ratio of EP neurons that are GFP+/mCherry- to neurons that are colabeled with TVA-mCherry and GFP (ie starter neurons). **E.** Sample image of striatum depicting dMSNs (*Drd1a-tdTom*, red) and RbV-GFP+ neurons (green) presynaptic to *Sst-Cre+* EP neurons. **F.** Quantification of the proportion of RbV-GFP+ neurons that were also positive for D1-tdTomato (D1-Tom+/RbV-GFP+ 530/539 cells, n=1 animal). **G, H.** Sample images of STN (G) and PF (H) from monosynaptic retrograde tracing, GFP+ cells are presynaptic to the indicated EP subpopulation. **I.** Brain-wide quantification of all regions where GFP+ neurons were found (excluding striatum). Data are presented as the number of cells found in a region divided by all cells counted in that animal (*Sst-Cre* n=3, *Pvalb-Cre* n=3, *Rbp4-Cre* n=3 mice). All data are represented as mean \pm SEM.

SUPPLEMENTAL ITEMS

Supp. Table 1 (related to Figure 1 and 2) (Suppl_Table_1.csv)

The average transcriptomes for all clusters described in Figure 1, and detailed analysis and comparisons of EP clusters 5 and 6.